■ **Surface Chemistry**

Water-Stable Zirconium-Based Metal–Organic Framework Material with High-Surface Area and Gas-Storage Capacities

Oleksii V. Gutov,[a] Wojciech Bury,[a, b] Diego A. Gomez-Gualdron,[c] Vaiva Krungleviciute,[d, e] David Fairen-Jimenez,[f] Joseph E. Mondloch,[a] Amy A. Sarjeant,[a] Salih S. Al-Juaid,[g] Randall Q. Snurr,*[c] Joseph T. Hupp,*[a] Taner Yildirim,*[d, e] and Omar K. Farha*[a, g]

Abstract: We designed, synthesized, and characterized a new Zr-based metal–organic framework material, **NU-1100**, with a pore volume of 1.53 ccg^{-1} and Brunauer–Emmett–Teller (BET) surface area of 4020 m^{2}g^{-1}; to our knowledge, currently the highest published for Zr-based MOFs. CH$_4$/CO$_2$/H$_2$ adsorption isotherms were obtained over a broad range of pressures and temperatures and are in excellent agreement with the computational predictions. The total hydrogen adsorption at 65 bar and 77 K is 0.092 g g^{-1}, which corresponds to 43 g L^{-1}. The volumetric and gravimetric methane-storage capacities at 65 bar and 298 K are approximately 180 v$_{STP}$/v and 0.27 g g^{-1}, respectively.

Well-defined metal–organic frameworks (MOFs) featuring molecular-scale pores and high internal-surface areas constitute a growing and remarkable chemically diverse class of materials of potential utility in a wide range of applications including catalysis,[1,2] gas separation,[3,4] sensing,[5] and storage.[6,7,8] In particular, MOFs have attracted much interest for on-board hydrogen or methane storage in vehicles. Both methane and hydrogen are promising candidates as replacements for gasoline (petrol). However, their compact storage in molecular form, especially in the case of hydrogen, remains a great challenge. Sorption or cryosorption in nanoporous materials is a promising way to lower the pressure required for storage of a given deliverable quantity of gas. Further practical requirements for on-

board applications include thermal, chemical, and mechanical stability (required for damage-free pelletization of the adsorbent; pelletization lowers back pressure during tank filling, thereby facilitating more rapid filling).

Over the last decade, significant progress has been made towards building new classes of MOFs with desired material characteristics. To a significant degree, MOFs can now be considered as programmable.[9] This circumstance has been achieved by tailoring the pore geometry and volume, surface area, and density of MOFs by the incorporation of different linkers and metal centers. Control over these parameters is crucial for constructing materials with high-capacity gas uptake, as well as stability. However, most known MOFs are not sufficiently stable to allow their application for gas storage in the presence of water.[10] To overcome this problem, we targeted Zr-based MOFs. These materials are known to possess high chemical and mechanical stability due strong ionic bonding between Zr^{4+} and carboxylate oxygen atoms.[11–15] However, Zr MOFs have been much less extensively investigated for hydrogen or methane storage than have many other MOF families.

Recent studies have demonstrated the feasibility of tuning the porosity of Zr-based MOFs by selective linker removal,[16,17] control over the framework topology, or ligand modifications.[18] These studies suggest that appropriate design of Zr MOFs can lead to materials with high surface area, a feature of exceptional importance for hydrogen storage at low temperatures.[6] Reticular synthesis, a methodology based on systematic extension of organic linkers between inorganic nodes, is the first choice approach for constructing MOFs with higher sur-

[a] Dr. O. V. Gutov,+ Dr. W. Bury,+ Dr. J. E. Mondloch, Dr. A. A. Sarjeant, Prof. Dr. J. T. Hupp, Prof. Dr. O. K. Farha
Department of Chemistry and International Institute for Nanotechnology
Northwestern University, 2145 Sheridan Road, Evanston, IL 60208 (USA)
E-mail: j-hupp@northwestern.edu
        o-farha@northwestern.edu

[b] Dr. W. Bury+
Department of Chemistry, Warsaw University of Technology
Noakowskiego 3, 00-664 Warsaw (Poland)

[c] Dr. D. A. Gomez-Gualdron, Prof. Dr. R. Q. Snurr
Department of Chemical & Biological Engineering
Northwestern University, 2145 Sheridan Road, Evanston, IL 60208 (USA)
E-mail: snurr@northwestern.edu

[d] Dr. V. Krungleviciute, Prof. Dr. T. Yildirim
NIST Center for Neutron Research
National Institute of Standards and Technology
Gaithersburg, MD 20899 (USA)

E-mail: taner@seas.upenn.edu

[e] Dr. V. Krungleviciute, Prof. Dr. T. Yildirim
Department of Materials Science and Engineering
University of Pennsylvania, Philadelphia, PA 19104 (USA)

[f] Dr. D. Fairen-Jimenez
Department of Chemical Engineering and Biotechnology
University of Cambridge, Pembroke Street, Cambridge CB2 3RA (UK)

[g] S. S. Al-Juaid, Prof. Dr. O. K. Farha
Department of Chemistry, Faculty of Science
King Abdulaziz University, Jeddah (Saudi Arabia)

[+] These authors contributed equally to this work.

🖥 Supporting information for this article is available on the WWW under http://dx.doi.org/10.1002/chem.201402895.

face areas and pore volumes than the prototypical structure in a MOF series. We sought to utilize this approach to design a new high surface area Zr MOF based on the **ftw** (4,12-connected net) topology.[19]

Herein, we designed and synthesized a highly porous Zr MOF, **NU-1100**, based on $Zr_6O_4(OH)_4^{12+}$ clusters and a pyrene-based tetratopic ligand 4-[2-[3,6,8-tris[2-(4-carboxyphenyl)-ethynyl]-pyren-1-yl]ethynyl]-benzoic acid (**L₄H**).

Two major design considerations in selecting the linker were: 1) the ligand should exhibit planar geometry to make the connectivity motif required for the **ftw** topology possible; and 2) the relative dimensions of the linker should be such that the four carboxylates define a rectangle that closely approximates a square, thereby enable the formation of cube-like boxes upon coordination to nodes. With this in mind, we designed ligand **L₄H** and computationally tested the possibility of its incorporation (as $\mathbf{L^{4-}}$) into the **ftw** topology. The initial model of the **NU-1100** structure was optimized by applying a procedure based on molecular energy minimizations described previously.[7] The resulting model demonstrated that $\mathbf{L^{4-}}$ can form a MOF with the desired topology without serious distortion of bond lengths and angles (Figure S3.1 in the Supporting Information).

The ligand **L₄H** was synthesized in four steps, including Sonogashira coupling reactions, followed by saponification of the resulting tetraester (Figure 1 a, for synthetic details, see the Supporting Information). The structure of **L₄H** was confirmed by single-crystal X-ray diffraction studies, which revealed the planar geometry of the molecules resulting in dense packing in the crystal structure (Figure S4.1 in the Supporting Information), which is commonly observed for conjugated systems.[20,21] Solvothermal reaction of **L₄H**, $ZrOCl_2 \cdot 8\,H_2O$ and benzoic acid (used as a modulator) in *N,N*'-dimethylformamide (DMF) at 120 °C gave a material with a powder X-ray diffraction (PXRD) pattern similar to that simulated for our preliminary computational model (Figure S3.2 in the Supporting Information), indicating the formation of a structure with the targeted **ftw** topology. Single crystals of **NU-1100** were obtained, and the structure was analyzed by means of single-crystal X-ray diffraction studies. The sample was found to have *Im-3* space group with an **ftw** topology;[19] to our knowledge, this represents the first example of isoreticular extension of the **ftw** topology. The structure of **NU-1100** consists of 12 connected $Zr_6O_4(OH)_4^{12+}$ nodes linked by planar tetratopic molecules of $\mathbf{L^{4-}}$ to form two types of pores (Figure 1 b and c). Ligand orientation is different in adjacent, rectilinear and nearly cubic, boxes, with two possible combinations of the box faces that finally form a "supercube" (Figure 1 c and d). Alternating orientations of the linker molecule in the crystal structure demonstrated a way for a twofold symmetrical ligand to be incorporated into a topology that, in principle, requires fourfold symmetrical ligands, resulting in a highly symmetric cubic space group.

Such an arrangement helps to compensate the small deviation of the linker periphery from a perfect square geometry (length-to-height ratios of the ligand carbon core are 0.96 and 0.97 in the crystal structures of **L₄H** and **NU-1100**, respectively).

The measured PXRD pattern of the **NU-1100** sample is in excellent agreement with the simulated pattern from single-crystal-structure data, confirming the single-phase nature of the bulk sample (Figure 2 a). Thermal gravimetric analysis (TGA) of the "as synthesized" material showed 60 % weight loss, corresponding to an equivalent accessibility by solvent molecules (Figure S5.3 in the Supporting Information). These initial results demonstrated the highly porous nature of the studied material. A TGA measurement of the **NU-1100** sample activated at 120 °C revealed stability up to 500 °C (Figure S5.3 in the Supporting Information). A small weight loss was observed above approximately 200 °C for both "as synthesized" and desolvated samples, corresponding to the elimination of water molecules from $Zr_6O_4(OH)_4^{12+}$ nodes.[16]

Computationally, **NU-1100** was predicted to have a large surface area and pore volume with high capacities for sorption of N_2, H_2, CH_4, and CO_2. To validate these predictions, we have
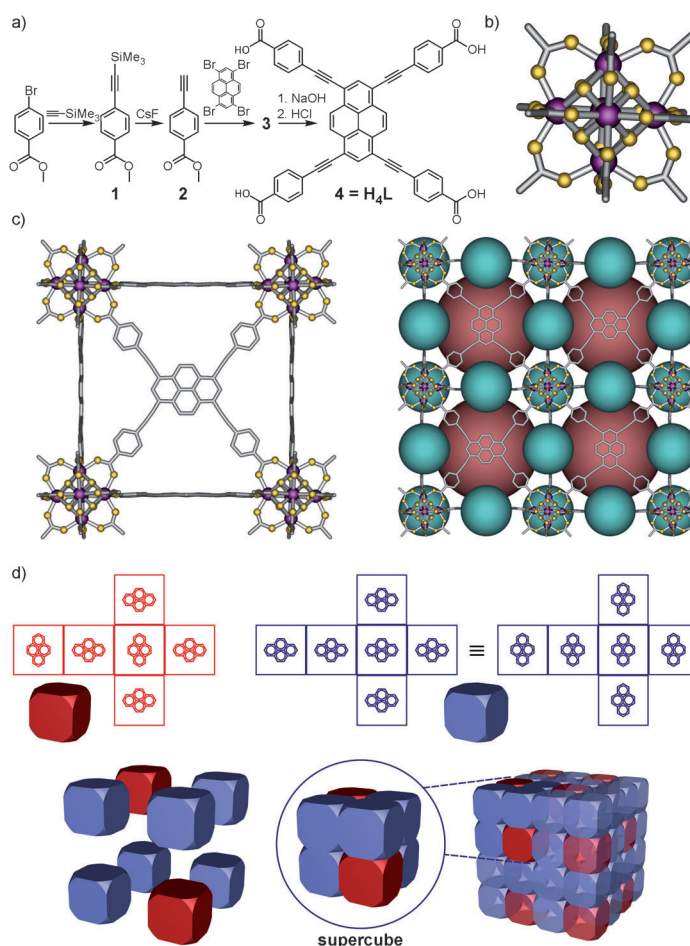

Figure 1. a) Scheme for **L₄H** synthesis. b), c) Structural elements and crystal packing of **NU-1100** (Zr atoms are shown as purple spheres, O atoms as yellow spheres, and carbon skeleton as gray sticks. Dark pink and light blue spheres occupy two major pore types in the crystal. d) Schematic representation of **NU-1100** supramolecular structure as a superposition of two different cubes (red and blue).
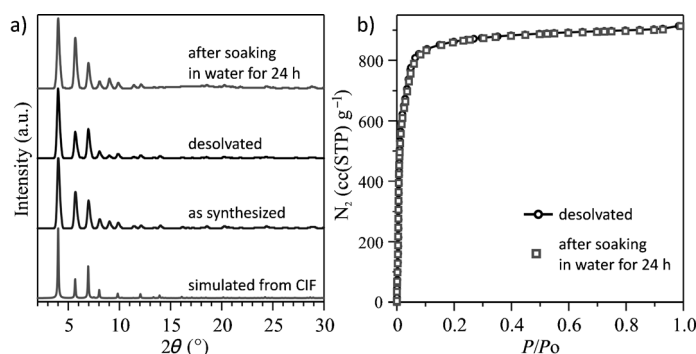
Figure 2. a) PXRD patterns of **NU-1100** after different treatments in comparison to the simulated pattern. b) N$_2$ adsorption isotherms of activated **NU-1100** at 77 K before and after immersion in water.

thermally activated a sample of **NU-1100** and studied its porosity by collecting nitrogen isotherms at 77 K, which were obtained independently at Northwestern University (NU) and the National Institute of Standards and Technology (NIST; for details, see the in the Supporting Information and Figure S5.4). Temperature-dependent high-pressure adsorption measurements were performed at NIST by using a computer-controlled Sievert apparatus, the details of which have been published elsewhere.[22] The experimental isotherms and resulting BET surface areas obtained at NU (Figure S5.7 in the Supporting Information) and NIST are very similar: 4020 m^{2}g^{-1} and 4060 m^{2}g^{-1}, respectively. These numbers are also in good agreement with the calculated value of 4333 m^{2}g^{-1} (Figure S5.8 in the Supporting Information) and represent, to our knowledge, the highest reported to date for Zr-based MOFs. The pore volume of **NU-1100**, derived from the obtained N$_2$ isotherm, is 1.53 cc g^{-1}, which is lower than the calculated value of 1.67 cc g^{-1} (78.1% porosity) by PLATON.[23] The pore-size distributions extracted from simulated and experimental isotherms by using the DFT method (Figure S5.6 in the Supporting Information) are in good agreement and showed the two pore types observed in the **NU-1100** crystal structure (Figure 1 c).

Besides its high thermal stability, **NU-1100** showed excellent stability against water, retaining its crystallinity and full porosity following soaking in liquid water for 24 h (Figure 2).

Figure 3 shows CH$_4$, CO$_2$, and H$_2$ adsorption isotherms over a wide range of pressures and temperatures. Low-temperature adsorption-isotherm data are indispensable, because they provide information on the maximum gas-storage capacity of the material. The excess H$_2$ isotherm at 77 K (Figure S6.1 in the Supporting Information) showed a shallow maximum uptake of 0.062 g g^{-1} near 45 bar and a slight decrease to 0.06 g g^{-1} at 65 bar. Consistent with this nearly flat excess isotherm, the total isotherm does not saturate with increasing pressure, reaching a very high value of 0.092 g g^{-1} at 65 bar (the highest pressure examined). The corresponding volumetric uptake is 43 g L^{-1}, among the highest values reported to date for H$_2$ storage (i.e., 35 g L^{-1} for **PCN-68**,[24] 36 g L^{-1} for **MOF-200**,[8] 41 g L^{-1} for **MOF-210**,[8] 47 g L^{-1} for **NU-100**,[7] and 49 g L^{-1} for **NU-111**[25] and **MOF-177**[26]). It is important to note that these

benchmark MOFs, such as **NU-100** and **MOF-177**, are based on copper paddlewheels or Zn$_4$O clusters, which are not as stable as the Zr-based **NU-1100**. Hydrogen uptake drops rapidly with increasing temperature. Nevertheless, **NU-1100** showed a non-negligible total uptake of 0.012 g g^{-1} at 298 K and 65 bar.

Additionally, **NU-1100** exhibited significant CO$_2$ uptake at high pressures. The maximum CO$_2$ uptake at 220 K is 37.3 mmol g^{-1}, which gives a pore volume of 1.42 cc g^{-1} (7% lower than that derived from nitrogen and methane). The CO$_2$ uptake at room temperature and 30 bar is approximately 26.2 mmol g^{-1}, corresponding to 70% of the total pore volume.

Methane-adsorption isotherms of **NU-1100** are shown in Figure 3. We obtained a maximum uptake of approximately 404 v$_{STP}$/v (38.6 mmol g^{-1}) at 125 K. This value effectively corresponds to the upper limit for the amount of gas that can be adsorbed under very high external pressures at ambient temperature. The observed maximum CH$_4$ uptake gave a pore volume of 1.54 cc g^{-1} (assuming liquid methane density at 125 K), which is in excellent agreement
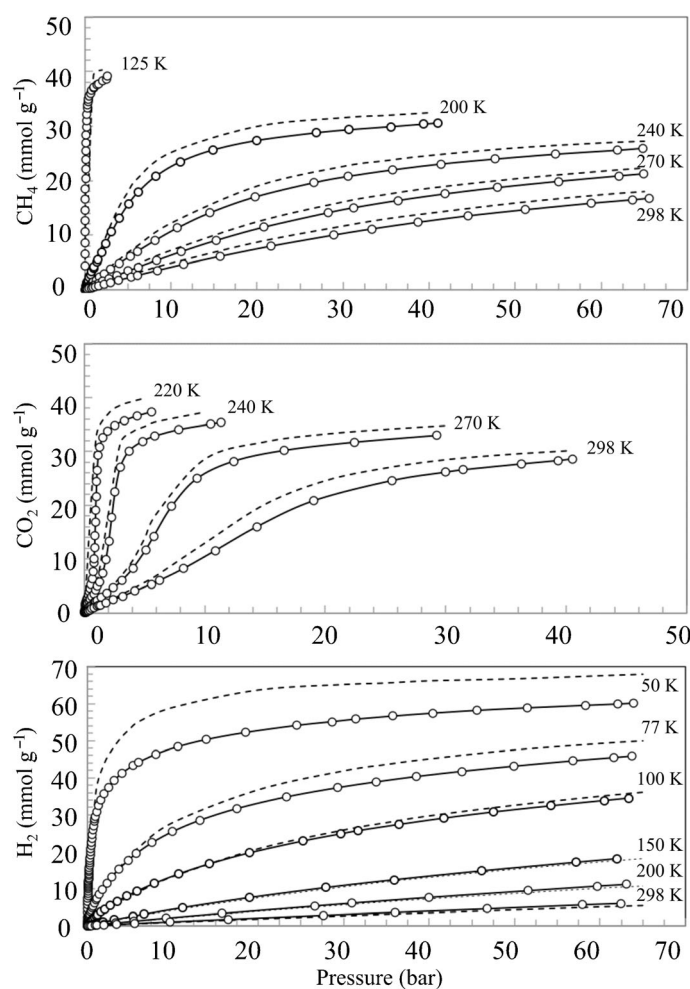

Figure 3. Total gravimetric gas-uptake isotherms for **NU-1100** at various temperatures. The lines with filled circles are experimental data, whereas the solid lines are simulated isotherms by using the Dreiding force field.

with the nitrogen pore volume. This suggests that methane is able to access most of the pores in **NU-1100** that are accessible to nitrogen at 77 K. The material has high volumetric and gravimetric methane-storage capacities at 65 bar and 298 K of approximately 180 v_{STP}/v and 0.27 g g^{-1}, respectively. Ultimately, the deliverable methane capacity determines the driving range of a natural-gas vehicle (NGV). In this case, it is important for a porous material to have low capacity in the approximately 5 bar range, and high capacity in the 60–70 bar range. The adsorption isotherm of **NU-1100** has a relatively shallow gradient at low pressure; taking 5 bar as the specific lower-pressure limit and 65 bar as the upper limit, the volumetric deliverable capacity of **NU-1100** is 156 v_{STP}/v at 298 K. This value is lower than that of **HKUST-1** (190 v_{STP}/v) and similar to other promising methane storage MOFs, such as **UTSA-20** (170 v_{STP}/v) and **PCN-14** (157 v_{STP}/v).[22] However, the advantages that **NU-1100** can offer are: 1) high gravimetric deliverable capacity (0.24 g g^{-1}), which is higher than in the abovementioned MOFs: 56 % higher than in **HKUST-1** (0.154 g g^{-1}), 75 % higher than in **PCN-14** (0.136 g g^{-1}), and 78 % higher than in **UTSA-20** (0.134 g g^{-1}); 2) high thermal stability; and 3) high water stability compared to the abovementioned MOFs. Simulated isotherms for CH$_4$, CO$_2$, and H$_2$ are in good agreement with the experimental data (Figure 3); however, there is a systematic overprediction of adsorption at all temperatures.[27]

Importantly, we have tested the cycling stability of **NU-1100**. Upon multiple cycles of methane adsorption/desorption, which are shown in Figure S6.7 in the Supporting Information, **NU-1100** showed no evidence for sample degradation (as was evident from the straight line fit with zero slope (green-dashed line)). The variation of the total adsorption at 65 bar is less than $\pm 2\%$, which is within the experimental error of our measurements.

To get better insight into the nature of the adsorption sites and gas-framework interactions in **NU-1100**, we extracted isosteric heats of adsorption (Q_{st}) from the absolute isotherms measured at different temperatures by using the Clausius–Clapeyron equation (details are given in the Supporting Information).

The results are summarized in Figure S7.4 in the Supporting Information, showing good agreement with simulated values. The magnitudes of the Q_{st} values for CH$_4$ and CO$_2$ are significantly smaller than in **UiO-66**, the prototypical Zr based MOF.[13,16] In the case of **UiO-66**, the Q_{st} for CO$_2$ varies from 28 to 24 kJ mol^{-1}, whereas in **NU-1100**, there is a sharp decrease from 25 to 16 kJ mol^{-1} at low loading. We attribute this initial Q_{st} value to the presence of OH groups from Zr clusters as the primary adsorption sites.[16] In the case of methane, **UiO-66** has a Q_{st} around 18–19 kJ mol^{-1}, whereas **NU-1100** showed a Q_{st} near 11 kJ mol^{-1}. However, for smaller gas molecules, such as H$_2$, Q_{st} is almost the same as in **UiO-66**. The initial Q_{st} of 5 kJ mol^{-1} is roughly constant over the whole H$_2$ loading range.

In conclusion, we have synthesized and characterized a highly porous and stable Zr-based MOF material **NU-1100**, which exhibited very promising gas uptake for hydrogen and natural-gas-storage applications. According to PXRD and sorption measurements, **NU-1100** demonstrated high stability against water. The total volumetric hydrogen adsorption at 65 bar and 77 K is 43 g L^{-1} (0.092 g g^{-1}), which places it among the best performing MOFs for hydrogen storage at low temperatures. The methane volumetric deliverable capacity of **NU-1100** between 65 and 5 bar is approximately 160 v_{STP}/v, which is comparable to those of the most promising methane-storage materials, but its gravimetric deliverable capacity (0.24 g g^{-1}) is significantly higher. These results, together with the possibilities to tune the porosity by ligand extension, establish **NU-1100** as a promising platform to further improve gas-sorption capacities in a highly stable MOF structure.

Acknowledgements

[1] J. Lee, O. K. Farha, J. Roberts, K. A. Scheidt, S. T. Nguyen, J. T. Hupp, *Chem. Soc. Rev.* **2009**, *38*, 1450–1459.

[2] C. Wang, J.-L. Wang, W. Lin, *J. Am. Chem. Soc.* **2012**, *134*, 19895–19908.

[3] Y.-S. Bae, A. M. Spokoyny, O. K. Farha, R. Q. Snurr, J. T. Hupp, C. A. Mirkin, *Chem. Commun.* **2010**, *46*, 3478.

[4] J.-R. Li, J. Sculley, H.-C. Zhou, *Chem. Rev.* **2012**, *112*, 869–932.

[5] L. E. Kreno, K. Leong, O. K. Farha, M. Allendorf, R. P. V. Duyne, J. T. Hupp, *Chem. Rev.* **2012**, *112*, 1105–1125.

[6] M. P. Suh, H. J. Park, T. K. Prasad, D.-W. Lim, *Chem. Rev.* **2012**, *112*, 782–835.

[7] O. K. Farha, A. Ö. Yazaydın, I. Eryazici, C. D. Malliakas, B. G. Hauser, M. G. Kanatzidis, S. T. Nguyen, R. Q. Snurr, J. T. Hupp, *Nat. Chem.* **2010**, *2*, 944–948.

[8] H. Furukawa, N. Ko, Y. B. Go, N. Aratani, S. B. Choi, E. Choi, A. O. Yazaydin, R. Q. Snurr, M. O'Keeffe, J. Kim, O. M. Yaghi, *Science* **2010**, *329*, 424–428.

[9] C. E. Wilmer, M. Leaf, C. Y. Lee, O. K. Farha, B. G. Hauser, J. T. Hupp, R. Q. Snurr, *Nat. Chem.* **2011**, *4*, 83–89.

[10] There are only a few known examples of MOFs stable in bulk water and in acidic solutions. These include: UiO-66-type, MIL-type MOFs, and Fe$_2$(BDP)$_3$ (BDP^{2-} = 1,4-benzenedipyrazolate): Z. R. Herm, B. M. Wiers, J. A. Mason, J. M. van Baten, M. R. Hudson, P. Zajdel, C. M. Brown, N. Masciocchi, R. Krishna, J. R. Long, *Science* **2013**, *340*, 960–964.

[11] J. E. Mondloch, W. Bury, D. Fairen-Jimenez, S. Kwon, E. J. DeMarco, M. H. Weston, A. A. Sarjeant, S. T. Nguyen, P. C. Stair, R. Q. Snurr, O. K. Farha, J. T. Hupp, *J. Am. Chem. Soc.* **2013**, *135*, 10294–10297.

[12] M. Carboni, C. W. Abney, S. Liu, W. Lin, *Chem. Sci.* **2013**, *4*, 2396–2402.

[13] V. Guillerm, F. Ragon, M. Dan-Hardi, T. Devic, M. Vishnuvarthan, B. Campo, A. Vimont, G. Clet, Q. Yang, G. Maurin, G. Férey, A. Vittadini, S. Gross, C. Serre, *Angew. Chem.* **2012**, *124*, 9401–9405; *Angew. Chem. Int. Ed.* **2012**, *51*, 9267–9271.

[14] J. H. Cavka, S. Jakobsen, U. Olsbye, N. Guillou, C. Lamberti, S. Bordiga, K. P. Lillerud, *J. Am. Chem. Soc.* **2008**, *130*, 13850–13851.

[15] D. Feng, W.-C. Chung, Z. Wei, Z.-Y. Gu, H.-L. Jiang, D. J. Darensbourg, H.-C. Zhou, *J. Am. Chem. Soc.* **2013**, *135*, 17105–17110.

[16] H. Wu, Y. S. Chua, V. Krungleviciute, M. Tyagi, P. Chen, T. Yildirim, W. Zhou, *J. Am. Chem. Soc.* **2013**, *135*, 10525 – 10532.

[17] M. J. Katz, Z. J. Brown, Y. J. Colón, P. W. Siu, K. A. Scheidt, R. Q. Snurr, J. T. Hupp, O. K. Farha, *Chem. Commun.* **2013**, *49*, 9449 – 9451.

[18] H.-L. Jiang, D. Feng, T.-F. Liu, J.-R. Li, H.-C. Zhou, *J. Am. Chem. Soc.* **2012**, *134*, 14690 – 14693.

[19] W. Morris, B. Volosskiy, S. Demir, F. Gándara, P. L. McGrier, H. Furukawa, D. Cascio, J. F. Stoddart, O. M. Yaghi, *Inorg. Chem.* **2012**, *51*, 6443 – 6445.

[20] O. V. Gutov, *Cryst. Growth Des.* **2013**, *13*, 3953 – 3957.

[21] O. V. Gutov, E. B. Rusanov, A. A. Kudryavtsev, S. G. Garasevych, O. V. Slobodyanyuk, V. M. Yashchuk, A. N. Chernega, *CrystEngComm* **2011**, *13*, 1373 – 1377.

[22] Y. Peng, V. Krungleviciute, I. Eryazici, J. T. Hupp, O. K. Farha, T. Yildirim, *J. Am. Chem. Soc.* **2013**, *135*, 11887 – 11894.

[23] PLATON, A. L. Spek Utrecht Univ., Utrecht, The Netherlands, 2000. Van der Waals radii [Å] used in the analysis C:1.70, H:1.2, Zr:2.36, O:1.52.

[24] D. Yuan, D. Zhao, D. Sun, H.-C. Zhou, *Angew. Chem.* **2010**, *122*, 5485 – 5489; *Angew. Chem. Int. Ed.* **2010**, *49*, 5357 – 5361.

[25] Y. Peng, G. Srinivas, C. E. Wilmer, I. Eryazici, R. Q. Snurr, J. T. Hupp, T. Yildirim, O. K. Farha, *Chem. Commun.* **2013**, *49*, 2992 – 2994.

[26] H. Furukawa, M. A. Miller, O. M. Yaghi, *J. Mater. Chem.* **2007**, *17*, 3197 – 3204.

[27] The origin of the overprediction may be related to inactivated regions as suggested by differences between measured and calculated pore volumes.